Journal of Wasit for Science and Medicine 2025: 18, (3), 1-12

# Advanced Biological Synthesis Techniques for Doped Cobalt Oxide in Combination with Titanium Dioxide: Methodological Insights and Potential Applications

**Enas Aliwy Razak, and Hanan Abd Ali Thjeel**

Department of Physics, College of Science, Wasit University, Wasit, Iraq

## Abstract

Anethum graveolens extract functions as a green reducing agent and stabilizing agent during the advanced biological synthesis process of cobalt-doped titanium oxide nanoparticles ($TiO_2$:0.3Co). The laboratory produced nanomaterials received detailed assessment through various structural, morphological, optical and electrochemical characterization methods. The XRD analysis verified $TiO_2$:0.3Co nanoparticles exist as highly crystalline structures with an average estimate of 29 nm for crystallite dimension. The spherical nanometer-sized particles had extensive clustering according to SEM and EDX analysis caused by nanoscale interparticle attractions. The presence of cobalt doping in the material structure reduced its optical band gap to 1.75 eV which increased its visible-light photocatalytic activity according to UV-Visible spectroscopy results. The chemical analysis through FTIR spectrometry validated metal-oxygen bond character through distinctive vibrational spectra which proved the structural stability of synthesized materials. The nanoparticles showed excellent glucose detection properties during electrochemical testing which suggests their practical use as biosensors. The extensive research shows an environmentally conscious synthesis method with high efficiency which makes $TiO_2$:0.3Co nanoparticles suitable for environmental cleanup operations and biomedical sensing.

**Keywords**: $TiO_2$ nanoparticles, green synthesis, cobalt.

## 1. Introduction

Nanotechnology advancements have driven an important transformation towards contaminant-free and highly efficient synthesis production methods which make biological fabrication a leading approach to creating complex nanostructured materials [1]. Investigate advanced approaches to

biological synthesis of doped cobalt oxide and titanium dioxide to investigate the combination of their electronic and magnetic and photocatalytic characteristics [2]. The synthesis process using plant extracts or microbial cultures as bio-derived reducing and stabilizing agents allows scientists to achieve specific control of nanoparticles through size measurements and morphology shaping and dopant distribution for material property adjustment in targeted applications [3]. The combination of titanium dioxide with doped cobalt oxide nanomaterials shows great promise to enhance photocatalysis along with energy transformation and cleaning processes due to enhanced band gap structures and better charge carrier separation [4]. Detailed studies on methodological aspects which optimize temperature conditions and pH levels and dopant amounts provide valuable information about the nucleation and growth procedures affecting the synthesis of complex nanocomposites that present a scalable manufacturing framework for advanced materials creation [5].

Anethum graveolens extract proves crucial for green chemistry through its complex collection of bioactive compounds that act both as reducing agents and surface stabilizer agents during nanomaterial synthesis [6]. During doped cobalt oxide combined with titanium dioxide synthesis the dill extract helps speed up metal ion reductions while guiding nanoparticle nucleation and growth to produce structurally enhanced dispersed nanoparticles [7]. The stable dispersion and improved functionality of nanoparticles results from functional groups in these biomolecules which also reduce material waste and hazardous chemicals during production [8]. This makes the procedure environmentally friendly. The extract contains innate biocompatibility features which make it suitable for biosensor applications [9]. These nanostructured materials provide outstanding capabilities for biosensor systems because they offer abundant surface and engineered electronic characteristics which allow efficient biomolecule fixing and better electron movement and enhanced detection performance toward biological substances. Anethum graveolens demonstrates excellent potential for advancing material synthesis together with biosensing technology through its dual operational capability [10].

## 2. Materials and methods

Titanium isopropoxide (TTIP), ethanol ($C_2H_5OH$), sodium hydroxide (NaOH), cobalt (Co), and plant extracts of Anethum graveolens were purchased and used in the current word.

### 2.1 Preparation of the plant extract

Fresh Anethum graveolens leaves were collected from the market and washed using deionized water. Then, leaves were dried for a week at room temperature and ground into fine powder. Leaves dried fine powdered 25g were added to 500 mL of deionized water to prepare the mixture. The resulting mixture was left at room temperature, protected from light for 24 hours and filtered using filter paper.

### 2.2 Preparation Co doped with ($TiO_2$) NPs

A solution of ethanol 50 mL, and deionized water 5 mL was stirred at 800 rpm and 50 °C for 10 minutes. Then, 10 mL of titanium isopropoxide (TTIP) was added and stirred for 30 minutes. After that, a 10 mL of plant extract was added and stirred for another 30 minutes. Subsequently, 0.3 g of cobalt (Co) was added and the mixture stirred for 60 minutes. Sodium hydroxide (NaOH) was added dropwise to adjust the pH to 7, causing a color change and thickening. The mixture was dried at room temperature for a week, ground, then calcined at 600 °C for two hours to obtain $TiO_2$:0.3Co nanoparticles.

## 3. Results and discussion

### 3.1 Structural Analyses (XRD, EDX, FE-SEM)

Powder X-ray diffraction (XRD) pattern shows distinctive peaks which identify cobalt and titanium oxide crystals as the $TiO_2$:0.3Co phase. The recognized X-ray peaks show correspondence to diffraction peaks (101), (311), (002), (222), and (302) at their respective locations of 25.54 °, 38.65 °, 48.10 °, 55.18 °, and 62.99 °, which align with the data from reference code 00-035-0793. The intense and accurate diffraction peaks indicate that the synthesized material shows a clear arrangement of crystalline structures. Synthesized nanoparticles show nanoscale crystallite sizes because the full width at half maximum (FWHM) values are measured at 0.18 ° to 0.72 °. Catalytic and surface reactivity performance was favored by the nanoscale dimension exhibited through crystallite sizes between 12.01 nm to 46.50 nm using Scherrer equation analysis. The average crystallite size measured 29.00 nm. Nanoscale crystallite size provides essential knowledge that directly affects material performance in photoactivity and detection, which strengthens its potential use in both biosensing and pollution treatment systems, as shown in (table 1) and (figure1).

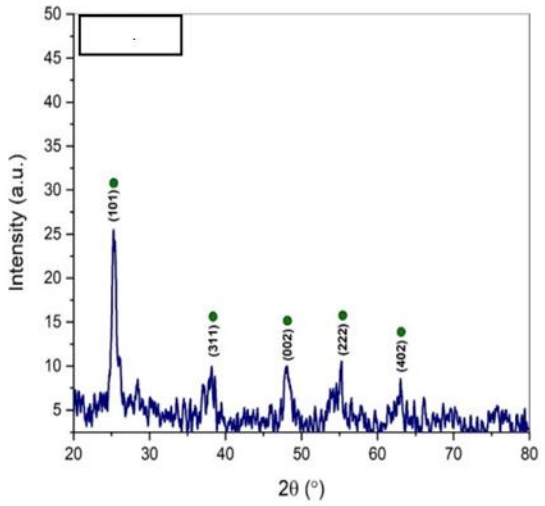


**Figure 1**: XRD pattern for cobalt titanium oxide.

**Table 1**: Structural parameters of cobalt titanium oxide.

| 2θ (Deg.) | FWM (Deg.) | Hkl | Crystals size (nm) | Average Crystals size (nm) | Referee code |
|---|---|---|---|---|---|
| 25.54 | 0.23 | 101 | 35.99 | 29.00 | 00-035-0793 |
| 38.65 | 0.18 | 311 | 46.50 | | |
| 48.10 | 0.72 | 002 | 12.01 | | |
| 55.18 | 0.36 | 222 | 24.75 | | |
| 62.99 | 0.36 | 402 | 25.73 | | |

The SEM images in (figure 2) present spherical cobalt titanium oxide nanoparticles which link together to form clusters or agglomerates. Different magnification levels in the micrographs show that nanoparticles display spherical features which have uniform shape and size differences. Nucleation together with particle growth takes place simultaneously during green synthesis through which nanoparticles end up clustering into aggregates because of dominating interparticle forces including van der Waals attractions and electrostatic interactions at nanometric scales [11, 12]. The EDX analysis shows a precise display of Co, O and Ti elements (not specifically labeled) and K in the sample composition. Potassium exists in synthesis-derived particles as unidentifiable residues or as remnants from synthesis methods. Additionally, gold peaks (Au) result from sample preparation for improved conductivity. Available data indicate that cobalt titanium oxide nanoparticles synthesized successfully due to their elemental composition with morphological characterization results [13].

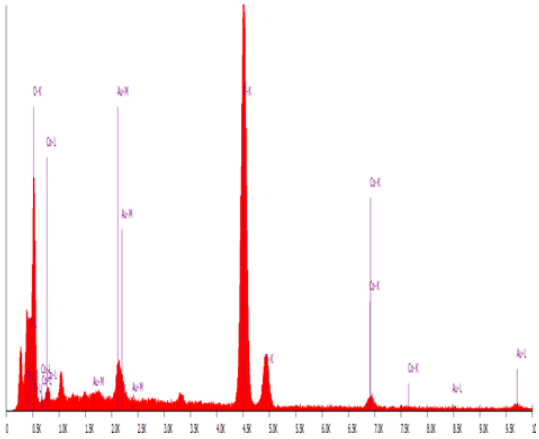

**Figure 2**: EDX analysis of cobalt titanium oxide.

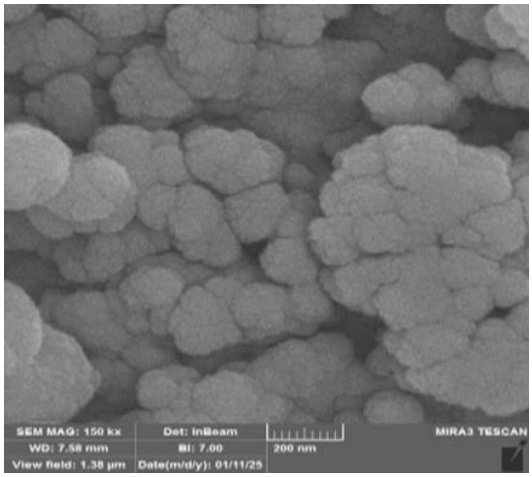


**Figure 3**: FE-SEM micrograph of cobalt titanium oxide (200 nm).

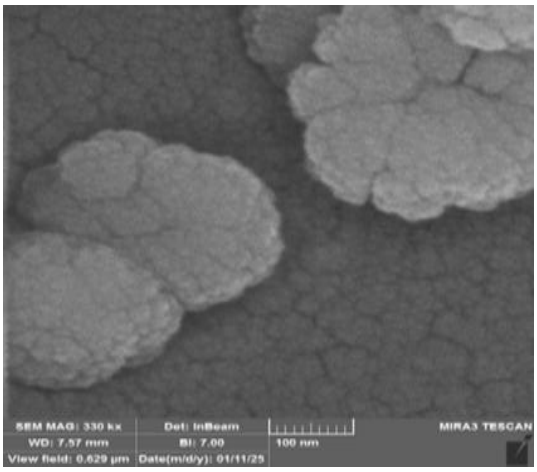


**Figure 4**: FE-SEM micrograph of cobalt titanium oxide (100 nm).

The SEM analysis provided supporting quantitative evidence about the shape distributions observed in the SEM illustrations. The analyzed particle sizes extend from 27 nm to 140 nm. The statistical analysis shows the average particle size reaches 62.36 nm and exhibits 27.26 nm standard deviation which describes wide particle size variations. The median value 59.43 nm is close to the mean suggests a nearly symmetric distribution with slight skewness toward larger sizes. The size dispersion of synthesized materials emerges from temperature instabilities and reaction duration and precursor concentrations and solvent parameters in the synthesis process, as shown in (table 2) and (figure 5).

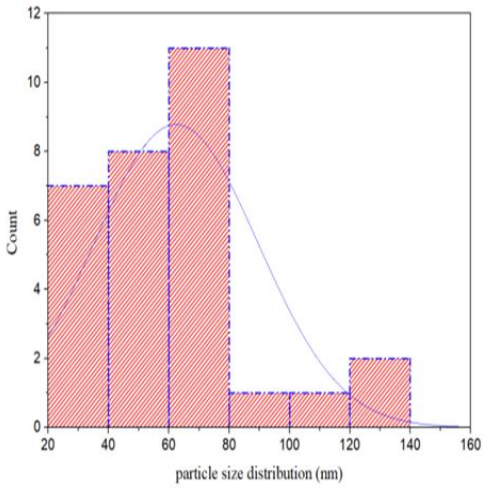


**Figure 5**: Particles size distribution.

**Table 2**: Statistical analysis of cobalt titanium oxide.

| | N Total | Mean | Standard Deviation | Sum | Minimum | Median | Maximum |
|---|---|---|---|---|---|---|---|
| G | 30 | 62.36077 | 27.26429 | 1870.823 | 27.801 | 59.4355 | 139.664 |

## 3.2 Optical properties results

The presented UV-Vis spectroscopy data illustrates the optical absorption characteristics of cobalt-doped titanium oxide nanoparticles ($TiO_2$:0.3Co). The Tauc

plot method helps determine the optical band gap by using absorption edge data from the absorption spectrum. The linear portion of the $(\alpha hv)^2$ versus hv data in the Tauc plot allowed researchers to calculate an optical band gap value of 1.75 eV. Through cobalt doping $TiO_2$ band gap absorbs less photon energy than the 3.2-3.4 eV range of pure $TiO_2$, indicating that cobalt doping structures the $TiO_2$ band gap with impurity levels or defect states, as shown in (figure 6). The material becomes better suited for visible light photocatalytic operations because dopant-induced alterations create electronic pathways that operate at reduced energy levels. The modified energy band gap demonstrates high importance since it enhances visible-light operation, which extends the application possibilities for $TiO_2$-based nanomaterials throughout environmental remediation and photovoltaic cell technology, as well as optoelectronics. The experimental findings demonstrate successful doping and electronic property modification of the nanostructures, which match previous scholarly reports about transition metal-doped titanium compounds [14, 15].

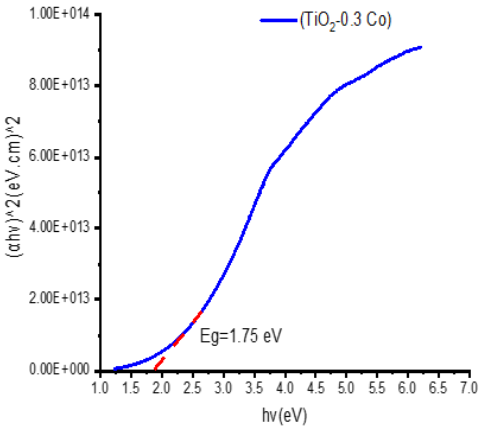


**Figure 6**: Energy band gab of cobalt titanium oxide.

## 3.3 FTIR spectrum analysis

The provided FTIR spectrum in (figure 7) of cobalt titanium oxide nanoparticles ($TiO_2$:0.3Co) shows important vibrational peaks that give information on the chemical environment of bonding and structural characteristics of the synthesized material. The intense absorption peak at approximately 419.10 $cm^{-1}$ is due to the metal-oxygen (M–O) stretching vibrations, which specifically indicate the presence of Co–O and Ti–O bonds characteristic of spinel or analogous oxide structures. The occurrence of this peak is a confirmation of the successful formation and crystallization of the metal oxide lattice. The second prominent absorption band at approximately 2166.38 $cm^{-1}$ can be due to the presence of adsorbed $CO_2$ or C≡O stretching vibrations, which is a common feature when samples are

exposed to the atmosphere during synthesis or storage. The occurrence of a broad band and comparatively high transmittance across most of the spectral range is indicative of the absence of any major organic impurities or adsorbed moisture, again indicating the purity of the synthesized oxide material. Overall, these observations are confirmation of the structural integrity and compositional accuracy of the cobalt titanium oxide nanoparticles, which is supported by literature reports and indicates successful formation of $TiO_2$:0.3Co structure.

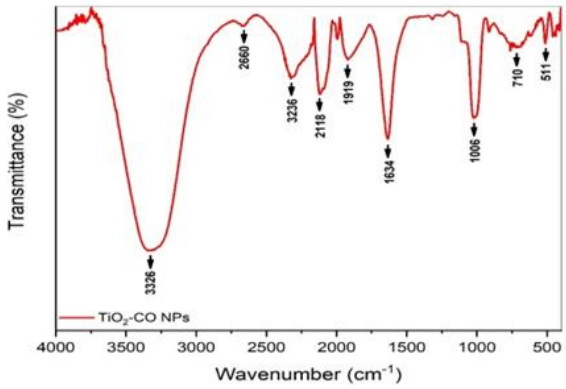


**Figure 7**: FTIR spectrum of cobalt titanium oxide.

## 3.4 Ramman spectrum results

The Raman spectrum of cobalt titanium oxide nanoparticles ($TiO_2$:0.3Co) (figure 8) provides shows vibrational modes corresponding to metal–oxygen bonds and crystalline lattice structures of the prepared material. The peak centered at about 219.33 $cm^{-1}$ is attributed to lattice vibrations typical of heavy metal ions (Co, Ti) in an oxide matrix, showing the successful development of the crystalline matrix. The remaining characteristic peaks at 641.98 $cm^{-1}$ and 917.74 $cm^{-1}$ can be attributed to bending and stretching vibrations of Ti–O and Co–O bonds, respectively, revealing clear metal-oxygen coordination. The intense peak at 1603.26 $cm^{-1}$ is generally due to the presence of graphitic or carbonaceous species, possibly due to surface contamination or residual organic precursors from the synthesis route. The band centered at about 2010.44 $cm^{-1}$ is most likely due to adsorbed species such as CO or $CO_2$ molecules weakly bound to the nanoparticle surfaces. Further, the series of peaks above 2400 $cm^{-1}$ up to 4300 $cm^{-1}$ generally depict overtones, combination bands, or fluorescence backgrounds, commonly observed for Raman spectra of metal oxide materials. The evident occurrence of these distinct vibrational bands supports the structural integrity and purity of the prepared cobalt titanium oxide nanoparticles, making the material suitable for various prospective applications in photocatalysis and energy storage technologies [16, 17].

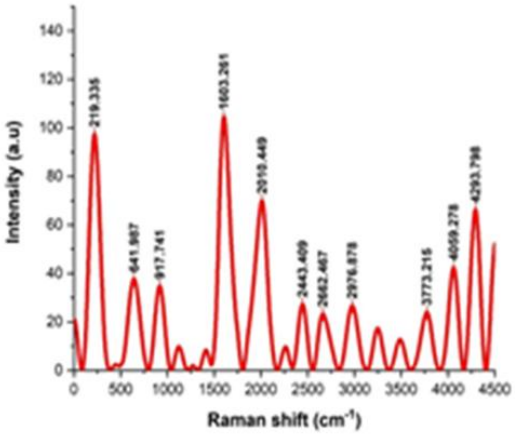


**Figure 8**: Raman spectrum of cobalt titanium oxide nanoparticles.

## 3.5 Photoluminescence (PL) characterization results

Photoluminescence (PL) characterization data (figure 9) clearly illustrate the photo-response behavior of cobalt titanium oxide ($TiO_2$:0.3Co) nanoparticles under illumination in the wavelength range of 300 to 900 nm. The intensity profile contains various peaks followed by valleys which demonstrate that the photo-response efficiency of nanoparticles changes according to wavelength. The photoactive characteristics of synthesized material are verified by strong reaction peaks at 400 nm in visible light wavelength range from 750 to 850 nm.

Research findings regarding optical band-gap determination support the conclusion that cobalt doping reduces $TiO_2$-based structure band gaps for enhanced absorption of visible light photons. The $TiO_2$:0.3Co nanoparticles exhibit appropriate charge transfer behavior under illumination, based on the measurements of recorded photocurrent intensity at 4.50 µA alongside the accumulated total charge reaching 2.16 µC over 60.2 seconds, as shown in (table 3).

The effective separation and transport of electron-hole pairs generated by photo incitation distinguishes $TiO_2$:0.3Co nanoparticles for photoelectrochemical and photocatalytic applications. The findings demonstrate that cobalt titanium oxide nanoparticles show great potential in solar energy conversion and environmental remediation as well as optoelectronic applications [18, 19].

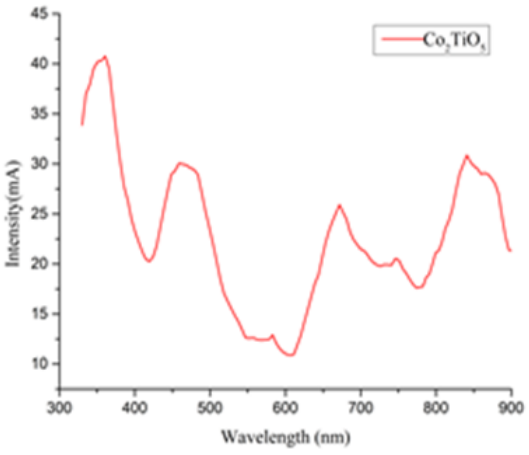


**Figure 9**: photoluminescence (PL) characterization curve.

**Table 3**: Photocurrent intensity properties.

| Index | Time/s | Height/A | Charge/C | Value /s |
|---|---|---|---|---|
| 1: level | 60.200 | 4.50E-06 | 2.16E-06 | 6.02E+01 |

The chronoamperometry curve for cobalt-doped titanium oxide ($TiO_2$:0.3Co) nanoparticles distinctly shows an immediate, sharp rise in current at approximately 60 seconds (peak at ~4.5 µA), indicating a fast and effective electrochemical response upon introducing a target analyte (such as glucose). This behavior confirms excellent sensitivity and rapid electron-transfer kinetics, highlighting the promising potential of $TiO_2$:0.3Co nanoparticles in electrochemical sensing and catalytic applications.

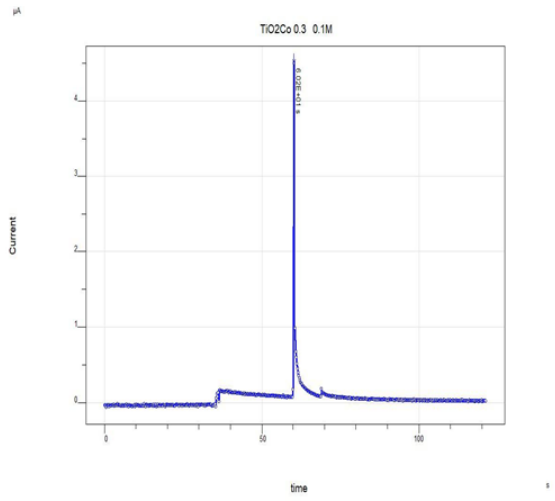


**Figure 10**: Chronoamperometry analysis.

The repeated cyclic voltammetry (CV) graph illustrates multiple cycles performed over time, reflecting consistent and reproducible electrochemical activity. The observed current peaks in anodic and cathodic regions remain stable across cycles, demonstrating high electrochemical stability and durability of the cobalt-doped $TiO_2$ nanoparticles. Such consistency is essential for practical applications, confirming that the synthesized material can reliably function as an electrochemical sensor for repeated analytical measurements.

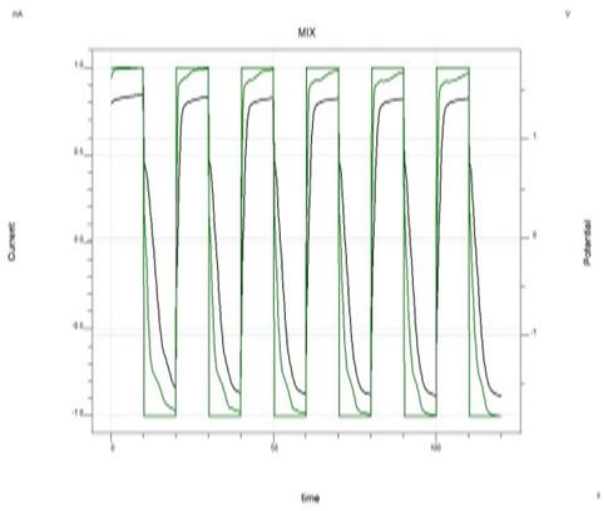


**Figure 11**: Repetitive cyclic voltammetry (CV) analysis.

The cyclic voltammetry comparison clearly shows changes in the electrochemical behavior of the cobalt-doped $TiO_2$ nanoparticles before (black curve) and after adding 0.1 M glucose (green curve). Notably, the glucose addition

resulted in enhanced anodic and cathodic currents, reflecting an increase in electrochemical activity. This enhancement confirms that cobalt-doped $TiO_2$ nanoparticles exhibit catalytic activity toward glucose oxidation, making them suitable candidates for glucose sensor development, especially in biomedical diagnostics.

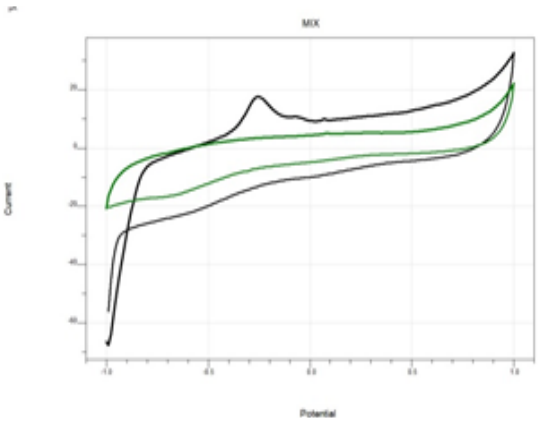


**Figure 12**: Cyclic Voltammetry (CV) Before and After Glucose Addition Black – before adding 0.1M glucose Green – after 0.1M glucose.

## 4. Conclusion

Biological synthesis of cobalt titanium oxide nanoparticles through Anethum graveolens extract yielded substantial improvements in material properties that include structure and optical characteristics as well as electrochemistry. The combination of XRD, SEM, and EDX and t optical band gap value of 1.75 eV. Tests verified the purity and crystallinity of nanoparticles after which optical tests revealed important electronic modifications which should improve photocatalytic and optoelectronic functionality. The synthesized nanoparticles maintained both strong electrochemical capabilities and displayed high responsiveness to glucose oxidation for biosensor applications. The green synthesis procedure developed in this work provides an industrial-scale framework for advanced nanotechnology that can enable $TiO_2$:0.3Co nanoparticle applications in multiple scientific and industrial applications.

## 5. References

1. Saleh H. M., and Hassan A. I., (2023). Synthesis and Characterization of Nanomaterials for Application in Cost-Effective Electrochemical Devices. Sustainability.15, 14, 10891.
2. Bakhshkandi R., and Ghoranneviss M., (2019). Investigating the synthesis and growth of titanium dioxide nanoparticles on a cobalt catalyst. Journal of Research in Science Engineering and Technology. 7, 4, 1-3.
3. Dikshit P. K., Kumar J., Das A. K., Sadhu S., Sharma S., Singh S., Gupta P. K., and Kim B. S., (2021). Green Synthesis of Metallic Nanoparticles: Applications and Limitations. Catalysts. 11, 8, 902.

4. Zhou H., Wang H., Yue C., He L., Li H., Zhang H., Yang S., and Ma T., (2024). Photocatalytic degradation by $TiO_2$-conjugated/coordination polymer heterojunction: Preparation, mechanisms, and prospects. Applied Catalysis B: Environment and Energy. 344, 123605.
5. Díez-Pascual A. M., Naffakh M., Marco C., Ellis G., and Gómez-Fatou M. A., (2012). High-performance nanocomposites based on polyetherketones. Progress in Materials Science. 57, 7, 1106-1190.
6. Ahmed R. S., Dahham A. M., Abdalameer N. K., and Mohammed R. S., (2024). Reduction of Silver Oxide Nanoparticles Using Anethum Graveolens Leaves Extract and Assessment of Their Antibacterial and Antibiofilm Properties. Research Square. [https://doi.org/10.21203/rs.3.rs-4689900/v1].
7. Lee H., Park Y. K., Kim S. J., Kim B. H., and Jung S. C., (2015). Titanium dioxide modification with cobalt oxide nanoparticles for photocatalysis. Journal of Industrial and Engineering Chemistry. 32, 259-263.
8. Sharma D., Kanchi S., and Bisetty K., (2019). Biogenic synthesis of nanoparticles: A review. Arabian Journal of Chemistry. 12, 8, 3576-3600.
9. Ul-Islam M., Alabbosh K. F., Manan S., Khan S., Ahmad F., and Ullah M. W., (2024). Chitosan-based nanostructured biomaterials: Synthesis, properties, and biomedical applications. Advanced Industrial and Engineering Polymer Research. 7, 1, 79-99.
10. Kaushal J. B., Raut P., and Kumar S., (2023). Organic Electronics in Biosensing: A Promising Frontier for Medical and Environmental Applications. Biosensors. 13, 11, 976.
11. Goldstein J. I., Newbury D. E., Michael J. R., Ritchie N. W., Scott J. H. J., and Joy D. C., (2017). Scanning electron microscopy and X-ray microanalysis. 4th Edition. Springer.
12. Shanker U., Vipin, and Rani M., (2023). Metal oxides-based nanomaterials: green synthesis methodologies and sustainable environmental applications. in Handbook of Green and Sustainable Nanotechnology: Fundamentals, Developments and Applications. Springer. 1-27.
13. Cullity B. and Stock S., (2014). Elements of X-Ray Diffraction, Pearson Education.
14. Hagfeldt A. and Graetzel M., (1995). Light-induced redox reactions in

nanocrystalline systems. Chemical reviews. 95, 1, 49-68.

15. Kumar S. G. and Devi L. G., (2011). Review on modified $TiO_2$ photocatalysis under UV/visible light: selected results and related mechanisms on interfacial charge carrier transfer dynamics. The Journal of Physical Chemistry A. 115, 46, 13211-13241.
16. Moon J., Li M., Ramirez-Cuesta A. J., and Wu Z., (2023). Raman Spectroscopy. Springer Handbook of Advanced Catalyst Characterization. Springer. 75-110.
17. Smith E. and Dent G., (2005). Modern Raman spectroscopy: a practical approach. John Wiley and Sons.
18. Grätzel M., (2001). Photoelectrochemical cells. Nature. 414, 6861, 338-344.
19. Linsebigler A. L., Lu G., and Yates J. T. Jr., (1995). Photocatalysis on $TiO_2$ surfaces: principles, mechanisms, and selected results. Chemical Reviews. 95, 3, 735-758.